J. Fluid Mech. (1973), *vol.* 61, *part* 3, *pp.* 417–447
Printed in Great Britain

Relaminarization in highly accelerated turbulent boundary layers

By R. NARASIMHA AND K. R. SREENIVASAN
Department of Aeronautical Engineering, Indian Institute of Science, Bangalore

(Received 15 September 1972 and in revised form 13 June 1973)

The mean flow development in an initially turbulent boundary layer subjected to a large favourable pressure gradient beginning at a point x_0 is examined through analyses expected *a priori* to be valid on either side of relaminarization. The 'quasi-laminar' flow in the later stages of reversion, where the Reynolds stresses have by definition no significant effect on the mean flow, is described by an asymptotic theory constructed for large values of a pressure-gradient parameter Λ, scaled on a characteristic Reynolds stress gradient. The limiting flow consists of an inner laminar boundary layer and a matching inviscid (but rotational) outer layer. There is consequently no entrainment to lowest order in Λ^{-1}, and the boundary layer thins down to conserve outer vorticity. In fact, the predictions of the theory for the common measures of boundary-layer thickness are in excellent agreement with experimental results, almost all the way from x_0. On the other hand the development of wall parameters like the skin friction suggests the presence of a short bubble-shaped reverse-transitional region on the wall, where neither turbulent nor quasi-laminar calculations are valid. The random velocity fluctuations inherited from the original turbulence decay with distance, in the inner layer, according to inverse-power laws characteristic of quasi-steady perturbations on a laminar flow. In the outer layer, there is evidence that the dominant physical mechanism is a rapid distortion of the turbulence, with viscous and inertia forces playing a secondary role. All the observations available suggest that final retransition to turbulence quickly follows the onset of instability in the inner layer.

It is concluded that reversion in highly accelerated flows is essentially due to the domination of pressure forces over the slowly responding Reynolds stresses in an originally turbulent flow, accompanied by the generation of a new laminar boundary layer stabilized by the favourable pressure gradient.

1. Introduction

What was possibly the first observation of a reversion from turbulent to laminar flow was in effect made by Taylor (1929) in his work on curved pipes; among the many other situations where such a reversion apparently occurs, the boundary layer subjected to a large favourable pressure gradient has been extensively studied in recent years (e.g. Launder 1964; Moretti & Kays 1965; Schraub & Kline 1965; Patel & Head 1968; Badri Narayanan & Ramjee 1969).

Authors	Criterion	Reynolds number	L	V
Schraub & Kline (1965)	Cessation of bursting	K^{-1}	U/U'	U
Patel & Head (1968)	Wall-layer velocity distribution	Δ_p^{-1}	U_*^2/p'	U_*
		Δ_τ^{-1}	$U_*^2\Big/\dfrac{\partial\tau}{\partial y}$	U_*
Bradshaw (1969)	Direct dependence on viscosity	Eddy Reynolds number	Dissipation-length parameter	$\tau^{\frac{1}{2}}$
Badri Narayanan & Ramjee (1969)	Decay of longitudinal velocity fluctuations	R_θ	θ	U

TABLE 1. Some proposed criteria for reversion

While procedures that are essentially empirical have been suggested for the prediction of boundary-layer characteristics during reversion (e.g. Jones & Launder 1972), there is as yet no agreement on the precise criterion for the occurrence of laminarization, or even on how its onset may be recognized. All current proposals for the critical parameter that might govern the phenomenon involve, however, the viscosity of the fluid, and most of them can be interpreted as some kind of Reynolds number: the different choices for the relevant length and velocity scales, say L and V, are summarized in table 1. ($U = U(x)$ is the free-stream velocity distribution, τ is the Reynolds shear stress and U_* the friction velocity; $U' = dU/dx$, $p' = -UU' = dp/dx$, and both p and τ are in kinematic units; θ is the momentum thickness.) Various combinations of K and the skin-friction coefficient c_f, of the form Kc_f^{-n} with n varying between $\frac{1}{2}$ and $\frac{3}{2}$, have also been suggested (Back, Massier & Gier 1964; Launder & Stinchcombe 1967).

There are particular difficulties with some of these proposals. For example, the bursting rate, if scaled with wall variables, decreases with the Reynolds number even in non-reverting constant-pressure flow (Rao, Narasimha & Badri Narayanan 1971); and it would be somewhat surprising if, over an appreciable Reynolds number range, the relevant parameter were to be one like K which takes no account of the shear flow at all (see §4.6). The last entry in table 1 implies, on the other hand, a vastly different mechanism, in which the sole effect of the pressure gradient would be to reduce the local Reynolds number R_θ to a 'critical' value. Patel & Head (1968) recognized clearly the potential importance of studying the effect of large pressure gradients on wall similarity; their attractive proposal, with which Bradshaw's is consistent under appropriate conditions, is based on a highly plausible mixing-length model for an equilibrium wall layer (Townsend 1961). However, the Patel–Head velocity profile derived from this model contains an algebraic error (see appendix A); use of the corrected velocity profile suggests that 'reversion' occurs at a 'critical' value for Δ_τ of only about $-0{\cdot}004$, which would no longer be in good agreement with Bradshaw's criterion. Furthermore the experiments of Patel & Head imply (as shown in appendix A) that reversion does not occur the first time either Δ_p or Δ_τ reaches its critical value, as quoted by them or corrected by us, so that there must be at least one other additional parameter in the problem.

Indeed, inferring reversion from the observed departure from a 'standard' turbulent law suffers from an inherent difficulty especially when the law is based on a fairly specific turbulence model; for the attempt presumes a completeness that has apparently not yet been achieved in our understanding of fully turbulent flow in pressure gradients. Thus, there is always the possibility that departures from the presumed standard may not so much be an indication of reversion as of our ignorance of turbulence. In contrast, the *completion* of the process can evidently be given a definite meaning, for it occurs, certainly for the mean flow field, when the net effect of the Reynolds stresses is negligible. Random fluctuations inherited from previous history may still remain, but are no longer relevant to the dynamics of the mean flow, which under these circumstances may aptly be said to have reached a quasi-laminar state. If (as indeed we shall argue) full laminarization is achieved only asymptotically, completion of the reversion process will of course have to be identified by specifying the degree to which the Reynolds stresses are negligible, but this is a matter of detail.

We therefore begin with a study that may be expected *a priori* to be valid during the later stages of reversion and involves the formulation of a 'quasi-laminar limit' with a suitable large pressure-gradient parameter (Sreenivasan & Narasimha 1971). The solution may be split into an inner viscous layer and an outer inviscid layer, so that its physical content has much in common with some earlier work (often in a different context) at both low and high speeds (e.g. Stratford 1959†; Vivekanandan 1963; Launder 1964; Head & Bradshaw (1971) have also used simplified inviscid flow arguments in their analysis of entrainment during reversion). However, our use of matched asymptotic expansions results in a theory which is not only more rational (cf. Van Dyke 1964) but also simpler (less computational effort) and more effective (e.g. choice of a virtual origin is not at all critical, unlike the case in Launder's calculations).

Using this solution as a kind of touchstone, we then proceed to sketch the other stages of the flow. Figure 1 illustrates a framework for the present analysis of the typical experimental situation, in which a fully turbulent boundary layer develops at constant pressure up to the point x_0, beyond which a steep pressure gradient is imposed. It is reasonable to begin by seeking a division of the flow, as shown in figure 1, into a region I in the neighbourhood of x_0 in which the flow continues to be 'fully turbulent', a region III sufficiently far downstream where the two-layer quasi-laminar limit is valid, a transitional region II in between, with an upstream boundary which, if well defined, could mark the onset of reversion, and finally a region IV where the flow is once again turbulent.

It would seem that region I should first be treated using one of the many sophisticated procedures now available for computing fully turbulent flows (see e.g. Kline, Moffatt & Morkovin 1969). We have not done this for two reasons. First, the validity of these procedures in large favourable pressure gradients remains undetermined, and will perhaps so remain till the intimately related question of possible reversion is resolved. The earlier remarks concerning inference of reversion apply again: in general, it will not be easy to decide whether differences

† From the present viewpoint, Stratford's work represents an ingenious but *ad hoc* attempt at second-order theory in a large *adverse* pressure gradient.

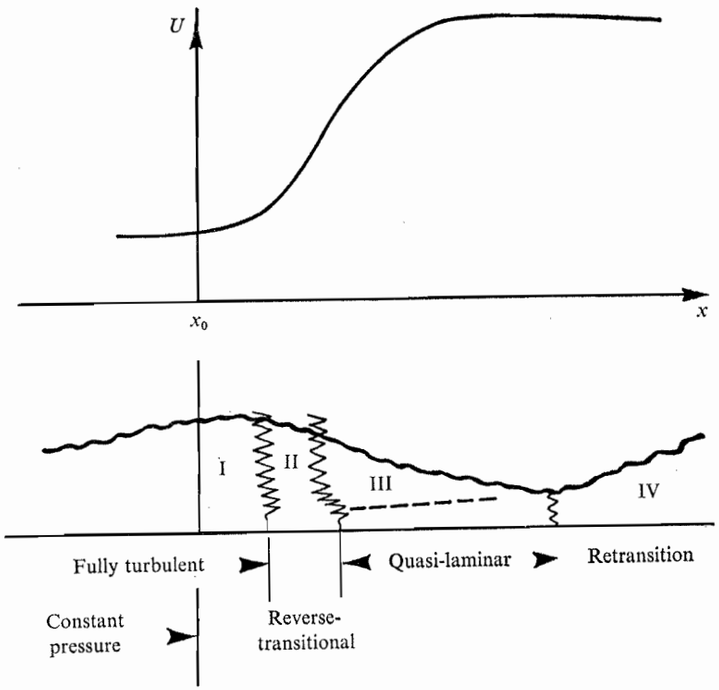

FIGURE 1. Sketch of the flow situation considered, with a preliminary division into different regions. The dashed line separates inner and outer layers in region III.

between measurement and prediction are due to relaminarization or to inadequacies in the turbulence model. Second, we find below that the quasi-laminar theory is valid almost from x_0 in the outer layer, so there is no strong need for more elaborate methods anyway. Our present purpose will therefore be served by illustrative calculations, which we make by the simple method due to Spence (1956). In fact, straightforward interpolation between limiting solutions seems to be adequate for a first approximation, and provides a basis for further refinement if necessary.

These analyses show that a rational division of the flow during reversion, into regions based on the dominating physical mechanisms, calls for considerable revision of the boundaries in figure 1; we shall show that there emerges a coherent overall picture of the phenomenon that largely explains experimental observations of *both* mean and fluctuating quantities.

2. The quasi-laminar equations

The development of an incompressible two-dimensional boundary-layer flow is governed by the equations

$$\partial u/\partial x + \partial v/\partial y = 0, \tag{2.1}$$

$$u\frac{\partial u}{\partial x} + v\frac{\partial u}{\partial y} = U\frac{dU}{dx} + \nu\frac{\partial^2 u}{\partial y^2} + \frac{\partial \tau}{\partial y}, \tag{2.2}$$

where u and v are mean velocity components along and normal to the main stream.

With the situation illustrated in figure 1, we now consider a limiting analysis for large values of the parameter $\Lambda \equiv -p'\delta/\tau_0$, where δ is a measure of the total boundary-layer thickness and τ_0 a characteristic Reynolds stress. We are therefore assuming that, on an elementary slice of the boundary layer between two successive stations x and $x+dx$, say, the net pressure force is much larger than the Reynolds shear force. Such an assumption does not necessarily violate the boundary-layer approximation, for two reasons. First, noting that

$$\Lambda^{-1} \sim c_f(U/U'\delta)$$

and that c_f is generally small, it is clear that both Λ^{-1} and $U'\delta/U$ can be small: the free-stream velocity does not have to vary rapidly over distances of order δ for Λ to be large. Second, there is no apparent tendency for the Reynolds stress to keep in step with a large pressure gradient, as measurements in wakes have shown (Narasimha & Prabhu 1972). In fact, values of $|\Lambda|$ appreciably greater than unity are easily obtained in many boundary-layer situations.

Of course in any real incompressible flow the pressure gradient cannot become large discontinuously, so a certain region $x = x_0+$ would, strictly speaking, have to be excluded from the limit. In the outer region of a turbulent boundary layer the viscous stresses are always negligible; a suitable outer limit of (2.2), as $\Lambda^{-1} \to 0$ with $\bar{y} = y/\delta$ fixed (bars denoting outer variables, but $\bar{u} = u$, $\bar{v} = v$, $\bar{x} = x$), is therefore

$$\bar{u}\frac{\partial \bar{u}}{\partial \bar{x}} + \bar{v}\frac{\partial \bar{u}}{\partial \bar{y}} = U\frac{dU}{dx}, \tag{2.3}$$

representing plane inviscid rotational flow, with the total head and vorticity present at x_0 being convected downstream along streamlines with no loss or diffusion. Towards the wall ($\bar{y} \to 0$), there will thus be a non-zero slip velocity given by

$$\bar{u}_0^2(x) = [U^2(x) - U^2(x_0)] + \bar{u}_0^2(x_0), \tag{2.4}$$

found from Bernoulli's equation along the zero streamline in the outer flow; the value of $\bar{u}_0(x_0)$ will be discussed in the next section.

The inner layer, which must develop near the wall to satisfy the no-slip boundary condition, is described by the limit $\Lambda^{-1} \to 0$ with $\tilde{y} = y/\tilde{\delta}$ fixed, where $\tilde{\delta}$, the inner-layer thickness, is $O(\Lambda^{-\frac{1}{2}}\delta)$: the corresponding limit of (2.2), with tildes denoting inner variables (again $\tilde{u} = u$, $\tilde{v} = v$, $\tilde{x} = x$), is the laminar boundary-layer equation

$$\tilde{u}\frac{\partial \tilde{u}}{\partial \tilde{x}} + \tilde{v}\frac{\partial \tilde{u}}{\partial \tilde{y}} = U\frac{dU}{dx} + \nu\frac{\partial^2 \tilde{u}}{\partial \tilde{y}^2}, \tag{2.5}$$

the Reynolds stress being ignored, as it can certainly be in the quasi-laminar region III of figure 1. Because the outer limit (2.3) is contained in (2.5), the division into two layers is not strictly necessary, but it is nevertheless both natural and instructive.

By conventional matching (e.g. Van Dyke 1964, p. 64), the boundary conditions are

$$\bar{u} \to U, \quad \bar{v} = 0 \quad \text{as} \quad \bar{y} \to \infty, \tag{2.6a,b}$$

$$\tilde{u}(x, \tilde{y} \to \infty) = \bar{u}(x, \bar{y} \to 0) = \bar{u}_0(x), \tag{2.6c}$$

$$\tilde{u} = 0 = \tilde{v} \quad \text{at} \quad \tilde{y} = 0. \tag{2.6d}$$

In an approximate method of calculation assuming a finite boundary-layer thickness δ, equation (2.6a) could be replaced by the condition

$$\overline{u} = U \quad \text{at} \quad \overline{y} = 1. \tag{2.6a'}$$

3. Method of solution

For solving the equations formulated above we adopt simple approximate methods, which prove to be entirely adequate.

3.1. *The outer equation*

Employing an integral technique, we need a parametric representation of the velocity profile that is sufficiently flexible to describe the initial fully turbulent boundary layer, to account for the slip velocity $\overline{u}_0$ and to characterize the expected laminar flow in the late stages of reversion. These multiple requirements unfortunately rule out a simple universal defect profile in which $(U-u)/(U-\overline{u}_0)$ is a function only of $\overline{y}$; experimental data in reverting flows confirm the expectation that a single such function cannot be valid in both turbulent and laminar flow. We have therefore tried expressions of the general type

$$\overline{u}/U = U_0(x) + A(x)\,\overline{y}^{n(x)} + \Sigma B_k(x)\,P_k(\overline{y}), \tag{3.1}$$

where $U_0 = \overline{u}_0/U$ is the non-dimensional slip velocity, the P_k are polynomials in $\overline{y}$, and A, n and B_k are parameters to be determined. The use of a power law leads to large slopes near the wall whenever $n < 1$, but these slopes become significant only at very small values of $y^+ \equiv yU_*/\nu$ (typically $\lesssim 5$). If therefore we ignore this region and follow the customary precaution of never differentiating a power-law profile, no difficulty is encountered.

In fact our experience is that the first two terms in (3.1), which together are equivalent to a single-parameter defect family

$$(U-u)/(U-\overline{u}_0) = F(\overline{y};\, n(x)), \tag{3.2}$$

are enough to give entirely satisfactory results. Sample calculations with a single additional term $B_1(x)\,\overline{y}$, to be quoted below, show that the results are hardly affected, so the last term in (3.1) will be generally ignored in the following.

Now, consistency of (3.1) with the standard power law used in turbulent boundary-layer calculations requires that $\overline{u}_0(x_0)$ and $U_0(x_0)$ be zero; from (2.4) and the boundary condition (2.6a') we must therefore have

$$1 - A(x) = U_0(x) = \{1 - [U(x_0)/U(x)]^2\}^{\frac{1}{2}}. \tag{3.3}$$

The two remaining parameters n and δ are obtained from the momentum and energy integral equations† (for an inviscid boundary layer!)

$$\frac{d\overline{\theta}}{dx} + \frac{U'}{U}(2\overline{\theta} + \overline{\delta}^*) = 0 \tag{3.4}$$

and

$$U^3\overline{\delta}^{**} = \text{constant}, \tag{3.5}$$

† A referee has suggested that it might be simpler to use an entrainment condition (see §4.1 below) instead of the energy equation (3.5).

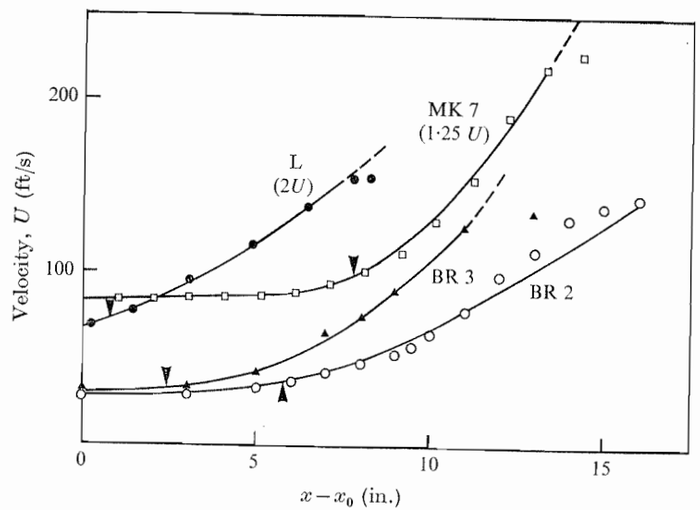

FIGURE 2. Free-stream velocity distributions in various reversion experiments, compared with values (full line) implied by best power-law fit to $\overline{u}_0$. Arrows mark K^*.

where

$$\left.\begin{aligned} \overline{\delta}^* &= \delta\int_0^1 \left(1-\frac{\overline{u}}{U}\right) d\overline{y}, \quad \overline{\theta} = \delta\int_0^1 \frac{\overline{u}}{U}\left(1-\frac{\overline{u}}{U}\right) d\overline{y}, \\ \overline{\delta}^{**} &= \delta\int_0^1 \frac{\overline{u}}{U}\left(1-\frac{\overline{u}^2}{U^2}\right) d\overline{y} \end{aligned}\right\} \tag{3.6}$$

are respectively the displacement, momentum and energy thicknesses of the outer layer. By straightforward algebra (3.6) can be evaluated in terms of n and δ, and δ eliminated between (3.4) and (3.5), to give a first-order nonlinear ordinary differential equation for n of the type

$$dn/dx = (U'/U) f(n, U_0), \tag{3.7}$$

which is written out in detail in appendix B. This equation is readily solved, using, for example, a Runge–Kutta routine with Gill's modification (Ralston & Wilf 1960, p. 110). Once n is known, δ is obtained from (3.5).

3.2. *The inner equation*

In most cases in the work reported below it was found possible to fit a power law of the form $\overline{u}_0 \sim (x-x_0)^m$ to the computed values of $\overline{u}_0$ and so obtain the inner solution as the appropriate member of the well-known Falkner–Skan family. For example, the skin-friction coefficient is given by

$$c_f = \tau_w/\tfrac{1}{2}U^2 = f''(0)\,[2(m+1)\,\nu/\overline{u}_0(x-x_0)]^{\frac{1}{2}}\,(\overline{u}_0^2/U^2), \tag{3.8}$$

where $f''(0)$ is the second derivative of the similarity solution f at the wall, with the same notation as in Rosenhead (1963, p. 235)†. The accuracy of such a procedure can be partly judged from figure 2, which compares, in some representative

† Equation (3.8) gives $c_f \sim (x-x_0)^{\frac{1}{2}(3m-1)}$, which goes to zero as $x \to x_0$ if $m > \frac{1}{3}$.

Reference	Flow code	Experimental configuration	x_0	R_θ at x_0	Remarks
Badri Narayanan & Ramjee (1969)	BR 1	Tunnel wall liner	7 in.	1650	BRn is experiment number n of the reference
	BR 2	Tunnel wall liner	4 in.	307	
	BR 3	Tunnel wall liner	7 in.	406	
	BR 4	40° wedge	0	2050	
	BR 5	40° wedge	0	1240	
	BR 6	40° wedge	0	777	
Blackwelder & Kovasznay (1972)	BK	Two-dimensional contraction	9·0 m	2500	—
Back & Seban (1967)	BS 1	Tunnel wall liner	4 in.	300	$U(x_0) = 52$ ft/s
	BS 2	Tunnel wall liner	4 in.	600	$U(x_0) = 110$ ft/s
Launder (1964)	L	Two-dimensional nozzle	18 in.	1000	
Launder & Stinchcombe (1967)	LS	Wedge	0	200	$K = 3 \times 10^{-6}$
Moretti & Kays (1965)	MK 5	Variable-height tunnel	2·267 ft		MKn is run n of the reference
	MK 7		2·011 ft	1410	
	MK 9		4·663 ft		
	MK 12		4·406 ft	2820	
Narahari Rao (unpublished)	NR	20° wedge	−4 in.	1590	Same basic apparatus as in BR
Patel & Head (1968)	PH 1	Centre body in pipe	−4 in.	2100	22 in. entry length
	PH 2	Centre body in pipe	−4 in.	6000	124 in. entry length
Schraub & Kline (1965)	SK	Water channel with a flexible wall	8·14 ft	586	Strong negative dp/dx
Sreenivasan (1972a)	S 1	40° wedge	11·5 in.	675	Same basic apparatus as in BR
	S 2	40° wedge	11·5 in.	1080	
	S 3	40° wedge	11·5 in.	850	

TABLE 2. List of flows analysed

cases, measured free-stream velocity distributions with those implied by the fit used for $\overline{u}_0$ in the calculations. (The experimental data are here designated by a code shown in table 2.) When such a fit was not good enough (as e.g. in BR 2, which represents the largest departure encountered in the present calculations), we have used the method of Thwaites (1949), which gives excellent results for the momentum thickness and skin friction but provides no velocity profiles.

Similarly the thermal characteristics of the boundary layer may be obtained by Lighthill's (1950) method. For example, in incompressible flow with a constant wall temperature T_0 and free-stream temperature T_∞, as in some of the experiments of Moretti & Kays (1965), the heat transfer from the appropriate inner solution with $\overline{u}_0 \sim (x-x_0)^m$ is given by the local Stanton number $S(x)$;

$$\frac{S(x)}{U_0} = \frac{q_0}{C_p \overline{u}_0 (T_0 - T_\infty)} = \frac{\alpha_m(\sigma)}{\sigma}\left[\frac{\nu}{\overline{u}_0(x-x_0)}\right]^{\frac{1}{2}}, \tag{3.9}$$

where q_0 is the wall heat flux, C_p the constant-pressure specific heat and $\alpha_m(\sigma)$ is a function whose values at a Prandtl number $\sigma = 0{\cdot}7$ (for air) have been tabulated against m by Curle (1962, p. 72). Again when the power law $\overline{u}_0 \sim (x-x_0)^m$ is not a sufficiently good fit to the experimental data, we have used a simple modification of the above method given by Curle (1962, pp. 76–77).

As mentioned in §1, calculations have also been made of boundary-layer development using the procedure of Spence (1956), which is straightforward and involves only simple quadrature.

4. Results

Unfortunately no single experiment (or set of experiments) provides a complete test case for the purposes of the present analysis, either because a significant quantity (like the skin friction) has not been measured or because the experimental conditions are not completely satisfactory (e.g. low Reynolds numbers). We have therefore examined, in the light of the analysis, all the data available to us, and made full calculations in those cases where the initial conditions were either known or easily guessed: these flows are listed in table 2, which serves to identify them and to indicate the experimental arrangement. A more detailed discussion of the available data is given in Sreenivasan (1972a).

Illustrative comparisons between experiment and theory are presented below for each flow quantity in turn, occasionally displaying the sensitivity of the theoretical results to some of the technical assumptions in the calculations. To help the reader in locating the flow stations relative to the imposed pressure gradient, various 'events' are often marked on the diagrams (key in §4.6). In particular the point where $K = 3 \times 10^{-6}$ (event K^*) is shown always, chiefly because of its convenience in characterizing the external pressure gradient independently of any boundary-layer measurement. (The one exception is flow L, for which Launder's values suggest K^* to be at x_0 itself.)

4.1. *Boundary-layer thickness*

This rather vague but useful quantity is defined here by $u(\delta)/U \approx \overline{u}(\delta)/U = 0{\cdot}995$ unless explicitly stated otherwise: clearly its experimental determination calls for accurate velocity measurements in the outer part of the boundary layer.† In the integral method of §3 we naturally put $u = U$ at $y = \delta$, but no inconsistency has been found in practice between these two definitions when the initial condition for the calculation of δ is taken as the 0·995 point in the measurements at x_0.

Figures 3(a) and (b) compare the boundary-layer thickness predicted by the present theory with various measurements. It is seen that choice of different velocity profile representations (figure 3a) or of a different virtual origin x_0 (involving a shift of 3 in. in BR 2, figure 3b) does not materially affect the calculations. The appreciable differences between computed and observed values of $\delta(x)$ for $x - x_0 > 9$ in. in BR 2, the largest encountered in the present calculations,

† The values of δ quoted here for the experiments of Badri Narayanan & Ramjee (1969) have generally been obtained from Ramjee (1968), except in a few cases where a re-examination of the raw data suggested the necessity for a revision.

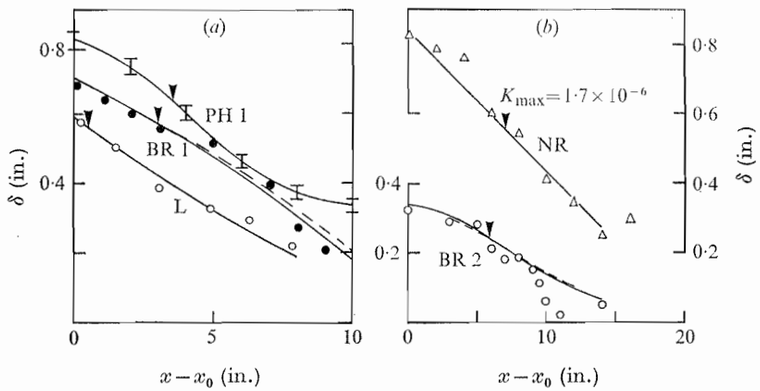

FIGURE 3. Boundary-layer thickness measurements (points) compared with calculations showing small effect of retaining the first term in the summation of the profile representation (3.1) with $n = \frac{1}{7}$ (dashed curve on BR 1), and of shifting the origin (downstream by 3 in., dashed curve on BR 2). Arrows mark K^*, except in flow NR.

suggest that the outer layer, with its relatively small velocity change $(U-\overline{u}_0)/U$, might have been missed in the measurements, particularly as the inner layer will have at this stage become relatively thick. This inference is supported by the good agreement between theory and experiment for inner-layer parameters (see §4.3 below) in the same flow, and for outer parameters in the very similar flow S 1 (§4.2). These comparisons for BR 2 are specially interesting because it is in a sense an extreme case; the low Reynolds number $R_\theta = 307$ at x_0 makes true, fully developed turbulent flow there unlikely.

Excellent agreement is also shown in figure 3(*b*) for flow NR, in which the maximum value of K ($\simeq 1{\cdot}7\times10^{-6}$) is appreciably less than the critical value suggested for example by Launder (1964) and Kline *et al.* (1967). In fact, all the comparisons in figure 3 demonstrate that the asymptotic theory constructed for a large Λ yields the boundary-layer thickness correctly almost right from x_0, where the pressure gradient is imposed: the neighbourhood of x_0 where the theory may not be valid cannot be distinguished.

The observed thinning of the boundary layer has a simple physical explanation in terms of vorticity conservation, which must hold in the outer limit (2.3). For it is a direct consequence of Bernoulli's equation (3.3) that the velocity difference $U-\overline{u}_0$ across the outer layer decreases downstream, requiring a corresponding contraction of the boundary layer to maintain the net outer-layer vorticity of about $(U-\overline{u}_0)/\delta$.

An immediate consequence of the inviscid nature of the outer flow is that the 'edge' of the boundary layer is a streamline and the entrainment is zero (to lowest order in Λ^{-1}). Head & Bradshaw (1971) have pointed out that it is important to consider both absolute and relative vorticity in discussing entrainment. According to the present theory, the absolute vorticity is constant (in the first inviscid approximation) along each outer streamline, and so is the value relative to the total outer-layer vorticity, which must also naturally be conserved;

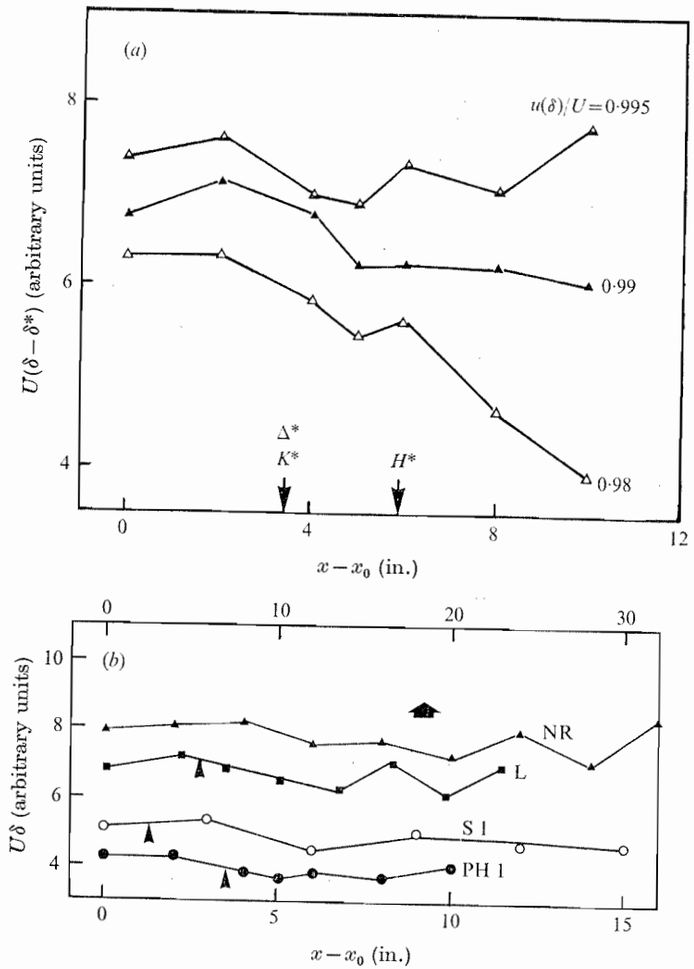

FIGURE 4. (*a*) Mass flux in boundary layer of flow PH 1, adopting three different definitions for δ. (*b*) Approximate constancy of the boundary-layer Reynolds number $U\delta/\nu$ during reversion; arrows mark K^*. Points are joined by lines for clarity.

but the value relative to the much higher overall vorticity (of order U/δ) must decrease. Experimental verification of such detailed results, or even of the conclusion that the mass flux $U(\delta-\delta^*)$ in the boundary layer must remain constant along the flow, is not easy especially as a definition of δ using vorticity requires differentiation of measured velocity profiles. However, experimental data for the mass flux, using more conventional definitions for δ (prescribing $u(\delta)/U$), leave no doubt (figure 4*a*) that the entrainment is negligible: indeed the conclusion is better confirmed for $u(\delta)/U$ closer to unity. Furthermore, as δ^* is generally small compared with δ in all these flows, an approximate but useful result is that the Reynolds number $R = U\delta/\nu$ changes little during acceleration from its initial value at x_0: figure 4(*b*) shows this to be well borne out by experiment.

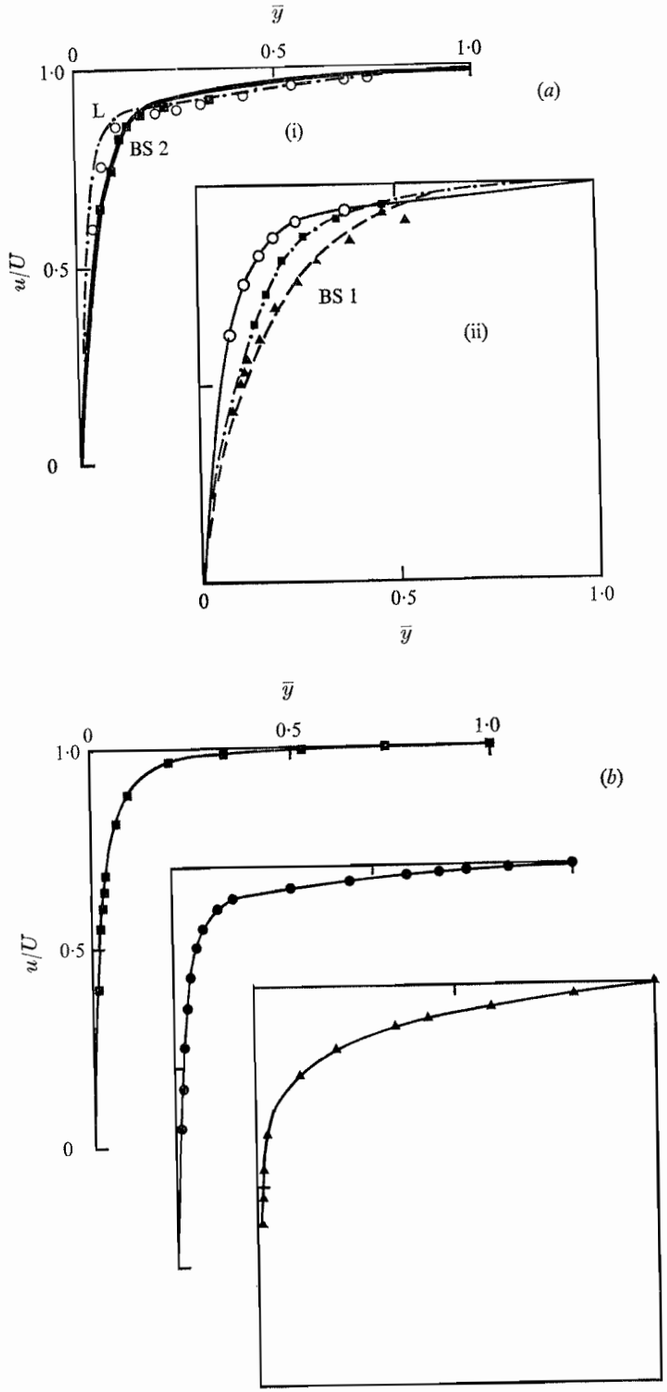

FIGURE 5. (*a*) Comparison of quasi-laminar solution (curves) with measured velocity profiles. (i) ○, flow L, $x = 21$ in.; ■, BS 2, $x = 0{\cdot}57$ ft. (ii) Flow BS 1: ○, $x = 0{\cdot}57$ ft; ■, 0·74 ft; ▲, 0·91 ft. (*b*) Comparison of quasi-laminar solution (full curves) with flow S 1. ▲, $x - x_0 = 0$ in.; ●, 6 in.; ■, 12 in.

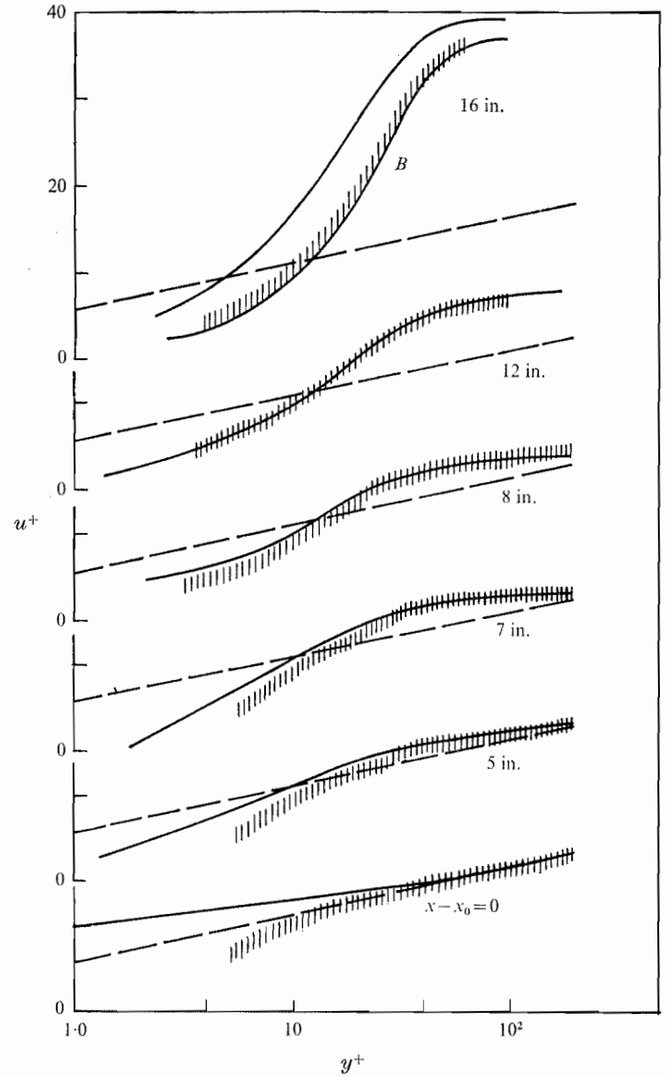

FIGURE 6. Velocity distribution in BR 2 on wall variables, using measured wall stress. /////, experimental data; ——, $u^+ = 5{\cdot}4 \ln y^+ + 5{\cdot}6$; ——, quasi-laminar theory, using Falkner–Skan inner solutions. At $x - x_0 = 16$ in. curve *B* shows the quasi-laminar theory with a Blasius inner solution.

4.2. *Velocity profiles: displacement and momentum thickness*

Once the inner and outer solutions are known, their union (in the manner described, for example, by Van Dyke 1964) provides the uniformly valid composite solution, to lowest order, and by integration of these profiles the displacement and momentum thickness can be determined. Alternatively, one can use the expressions

$$U\delta^* \approx U\bar{\delta}^* + \bar{u}_0\tilde{\delta}^*, \quad U^2\theta \approx U^2\bar{\theta} + \bar{u}_0^2\tilde{\theta}, \tag{4.1}$$

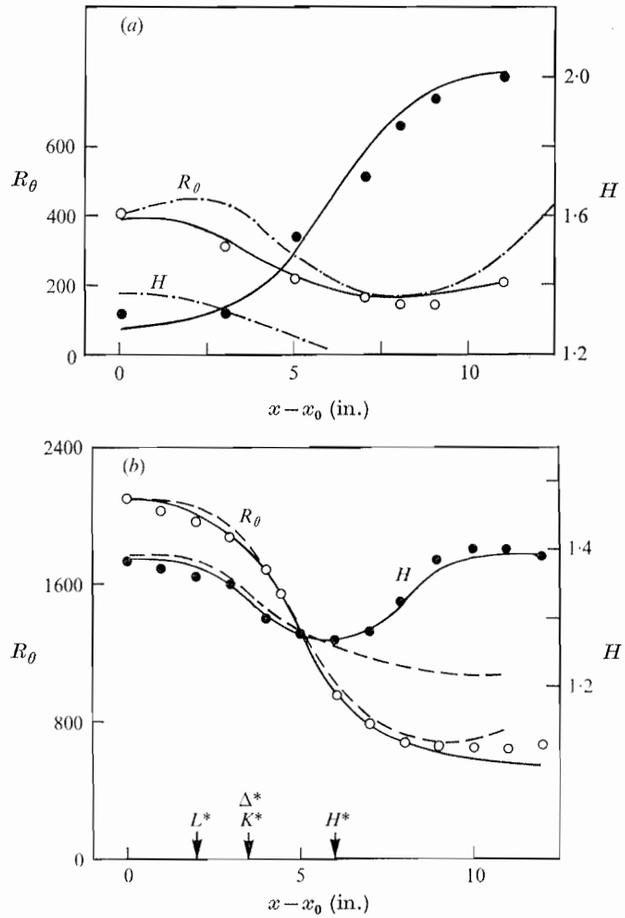

FIGURE 7. Reynolds number and shape factor in (*a*) BR 3 and (*b*) PH 1. ——, quasi-laminar theory; —·—·—, fully turbulent flow, using Spence's method.

derived easily from the standard definitions of δ^* and θ by expanding the uniformly valid expression for u in the integrand in terms of the inner and outer solutions and retaining the lowest order terms. (Note incidentally that, while we must have $\tilde{\delta} \ll \delta$ for the asymptotic analysis to be valid, contributions to δ^* or θ from both solutions can be of the same order if $(U-\overline{u}_0)/U$ is small, for then we can have

$$U\delta^* = O[(U-\overline{u}_0)\,\delta] = O[\overline{u}_0\tilde{\delta}^*],$$

still keeping $\tilde{\delta}$ (always of order $\tilde{\delta}^*$) much less than δ; similarly for θ.)

Figures 5 (*a*) and (*b*) show excellent agreement between measured and predicted velocity profiles in outer variables, especially for the flow studied by Sreenivasan (1972*a*) with the object of obtaining accurate outer-layer distributions. The more severe test imposed by the use of wall variables for plotting data (figure 6, for flow BR 2) shows, not unexpectedly, certain discrepancies near the wall in the early stages of reversion ($x-x_0 < 7$ in.), even when the measured wall stress is

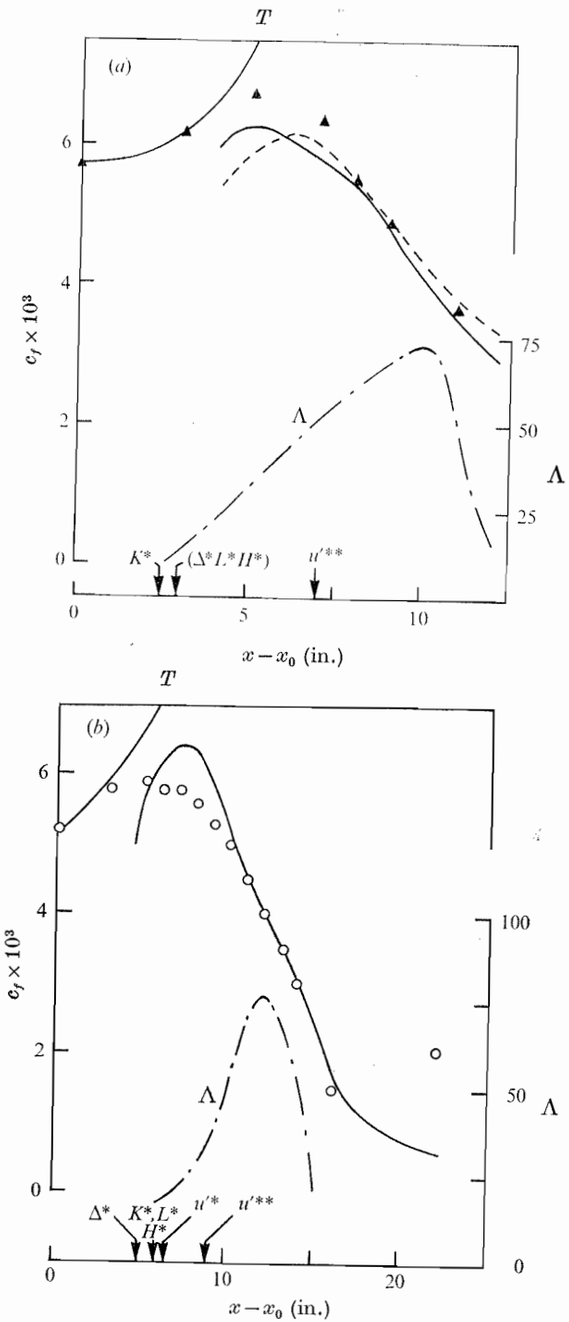

FIGURE 8. Skin friction and pressure gradient parameter in BR 3 and (*b*) BR 2. c_f first follows the curves marked T, obtained from a fully turbulent calculation using Spence's method; downstream, it obeys quasi-laminar theory (——, Thwaites's methods; – – –, Falkner–Skan method). Note in (*b*) the large departure of measured c_f from theory at the last station, indicating retransition to turbulence.

used for defining the variables. At the last station $x-x_0 = 16$ in., the pressure gradient has dropped to zero, so that the Falkner–Skan fit to $\overline{u}_0$ at earlier stations is no longer valid (figure 2); as laminar velocity profiles form a one-parameter family to a good approximation, a 'local' Blasius solution (i.e. one fitted to the local momentum thickness, for example) for the inner problem is more appropriate, and produces excellent agreement.

Whatever discrepancies there might be close to the wall just downstream of x_0, however, apparently they have no great effect on the integral parameters of the velocity profile like R_θ and the shape factor $H = \delta^*/\theta$; both of these are very well predicted (figures 7 and 8), again almost all the way from x_0, in flows with a relatively low initial Reynolds number and high final value of H (BR 3, figure 7*a*) as well as in the opposite case (PH 1, figure 7*b*).

Also shown on figures 7 (*a*) and (*b*) are the values of R_θ and H in fully turbulent flow as given by Spence's method: it is seen that these agree with the quasi-laminar solution over the initial stages for H (up to its minimum), and much farther downstream for R_θ. The explanation for this somewhat surprising result is that with a large pressure gradient the skin-friction term in the momentum integral equation solved by Spence's method does not make a large contribution to the momentum balance in any case, so that the solution approximates to that of (3.4) in the earlier stages of reversion where the boundary-layer characteristics are dominated by the outer flow (as the terms containing $\overline{u}_0$ in (4.1) are small).

4.3. *Wall parameters*

The most extensive (and also possibly the most reliable) measurements of the skin friction during reversion have been made in two flows BR 2 and BR 3, using a heat-transfer gauge with a universal calibration in both laminar and turbulent flow. Comparison with the inner-layer calculations of §3.2 shown in figures 8 (*a*) and (*b*) reveals generally good agreement in the later stages of reversion, particularly when using the Thwaites method, which has a slight superiority over the Falkner–Skan solutions owing to the difficulty in fitting a uniform power law to $\overline{u}_0$ (see figure 2). It is consistent with our observation on the inner velocity profile (§4.2) that the quasi-laminar solution (3.8) for c_f should be invalid in the earlier stages of flow development; the reason is not merely that associated with the failure of boundary-layer theory at the leading edge of, say, a flat plate, but also that the Reynolds stresses are not in fact negligible in the wall layer near x_0. Thus, calculations using Spence's method for fully turbulent flow predict quite well the observed initial increase in c_f. These two limiting solutions do leave a definite although short region in the middle which could legitimately be identified as the transition region II of §1.

A second wall parameter on which experimental information in reverting flows is available is the heat-transfer coefficient measured by Moretti & Kays (1965). A typical set of results, shown in figure 9, reveals again a transition region between fully turbulent and quasi-laminar flows, of the same nature as in c_f. Similar comparisons with three other experiments (MK5, MK9, and MK12) confirm the above conclusions (Sreenivasan & Narasimha 1971).

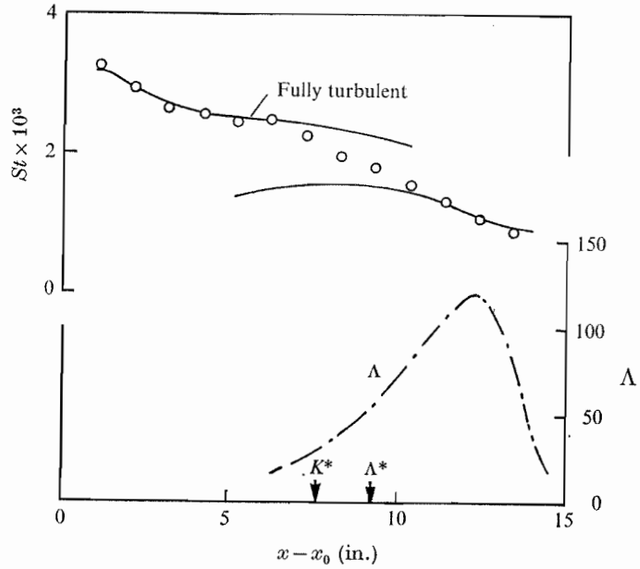

FIGURE 9. Comparison between measured (circles) and calculated (curves) variation of Stanton number in MK 7. The fully turbulent curve is taken from Moretti & Kays (1964).

4.4. *The pressure-gradient parameter*

Because of the likely correlation of at least the final stages of reversion with the parameter Λ, it would be useful to have its value at each station, x, but this is not directly possible because Λ involves the unknown characteristic Reynolds stress τ_0. This difficulty is not very serious, however, because there are grounds for believing that during rapid acceleration τ_0 hardly changes in magnitude (Launder 1964); such 'stress-freezing' has been observed by Narasimha & Prabhu (1972), for example, in suddenly accelerated wakes, and is consistent with the measurements of turbulent energy reported by Blackwelder & Kovasznay (1972). We may thus replace the local stress $\tau_0(x)$ by the initial value $\tau_0(x_0)$, which in turn may be approximated by the wall stress $\tau_w(x_0)$ at x_0 as the boundary layer may be assumed to be in equilibrium there. The parameter

$$\Lambda(x) = -p'(x)\,\delta(x)/\tau_w(x_0)$$

so calculated is shown in figures 8 and 9, $\tau_w(x_0)$ being obtained from a standard curve such as that of Coles (1953) if necessary (as for example, in the Moretti & Kays experiments).

4.5. *The 'turbulent' velocity fluctuations*

Here again we need to consider inner and outer layers separately. Badri Narayanan & Ramjee (1969) observed that, during the later stages of reversion, the distribution of the r.m.s. value of the fluctuating longitudinal velocity component u' exhibited, near the wall, a certain similarity, in terms of 'internal' scales like the location ($y = l$) and magnitude ($u'_{\max}$) of the maximum value of u' at each

station. No attempt was, however, made to relate these scales to other parameters in the problem.

Now if the u' fluctuations in the quasi-laminar flow are largely an inheritance from the initial turbulent boundary layer and not due to local generation, the frequencies contributing most to the energy will be appreciably less than the value $\overline{u}_0/\tilde{\delta}$ characteristic of the inner layer. For example, at $x = 16$ in. in BR 2,

$$\overline{u}_0/\tilde{\delta} \simeq U/\tilde{\delta} \simeq 20\,000 \text{ c/s},$$

whereas observation shows that there is little energy beyond frequencies of the order of 10^3 c/s in u'; such fluctuations are therefore quasi-steady to a good approximation.† Now the development of steady perturbations on a laminar boundary layer that is a member of the Falkner–Skan family has been studied in great detail by Chen & Libby (1968), who have formulated and solved the appropriate eigenvalue problems. Their results for the decay of the perturbation imply that, sufficiently far downstream, we should have $l(x)$ scaling with $\tilde{\delta}(x)$ and

$$\frac{u'_{\max}}{\overline{u}_0} \propto (x - x_0)^{-\frac{1}{2}(1+m)\lambda_1}, \tag{4.2}$$

where $\lambda_1 = \lambda_1(m)$ is the lowest eigenvalue computed by Chen & Libby for the boundary layer with $\overline{u}_0 \propto (x - x_0)^m$.

Data on these quantities from the experiments in which a power-law fit to $\overline{u}_0$ was particularly good are shown in figures 10(*a*) and (*b*). Although there is considerable scatter in the data for l, chiefly because of the difficulty of determining the location of a maximum that occurs very close to the wall, it is clear that the mean trend of the parameter $l/\tilde{\delta}$ is independent of x. The velocity scale $u'_{\max}$ is capable of more accurate determination and follows the power-law decay of (4.2) very closely (figure 10*b*). Incidentally, using Chen & Libby's data on λ_1 the exponent in (4.2) is well fitted by the expression

$$-\tfrac{1}{2}(1+m)\lambda_1 = -(1+3{\cdot}1m) \tag{4.3}$$

for $m > 0$, and in the experiments surveyed here is not far from -6.

This mechanism naturally cannot operate in the outer layer, where conditions appear to be akin to those under which the theory of rapid distortion might apply. Although an appropriate version of this theory for anisotropic shear flow is not yet available, we note that the shear in the outer layer is usually negligible, and recent work on axisymmetric homogeneous turbulence (Sreenivasan 1972*b*) suggests that, unless conditions are extreme, the isotropic results of Batchelor & Proudman (1954) provide good estimates of the change in component energies. Now the rapid-distortion limit ignores both inertia and viscous forces, and can be valid only if the final position of each particle is determined by the external strain (i.e. pressure gradient in the present case) to within a distance less than a characteristic scale of the turbulence. If this scale is taken as the Kolmogorov length, the condition is not easily satisfied; but useful results can be obtained

† We may also recall here the finding of Launder (1964) that the measured absolute energy contained above any particular wavenumber continuously decreases during acceleration.

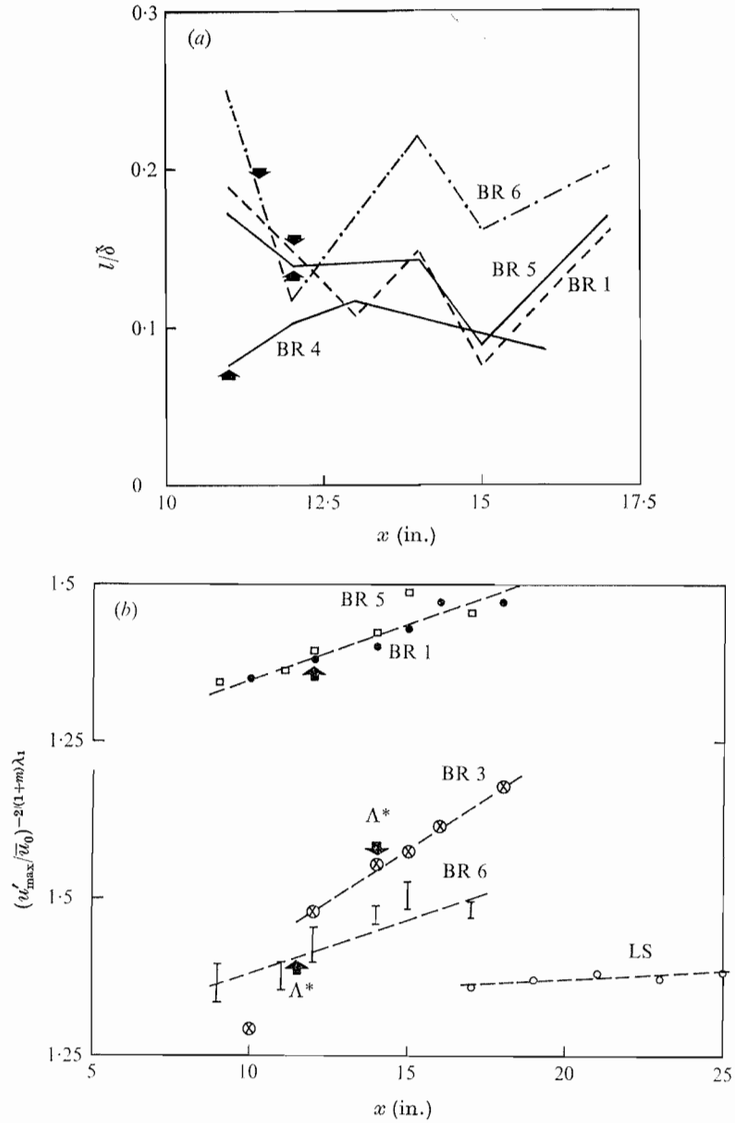

FIGURE 10. (*a*) Length scale in similarity distribution of u'. (*b*) Decay of velocity fluctuations in quasi-laminar regime. ●, BR 1; □, BR 5; ⊗, BR 3; ⌶, BR 6; ○, LS. Arrows mark Λ*, which cannot be located in LS because δ is not known. No significance need be attached to the single curve drawn through the points for BR 1 and BR 5, which happen to plot very closely together.

by the theory even when the condition is met only for the energy-containing eddies (Townsend 1956, p. 66). Taking the latter as having a scale of order δ, calculation shows that the time of flight of a particle in the outer layer is approximately a fifth to a tenth of δ/u', in the experiments of Badri Narayanan & Ramjee

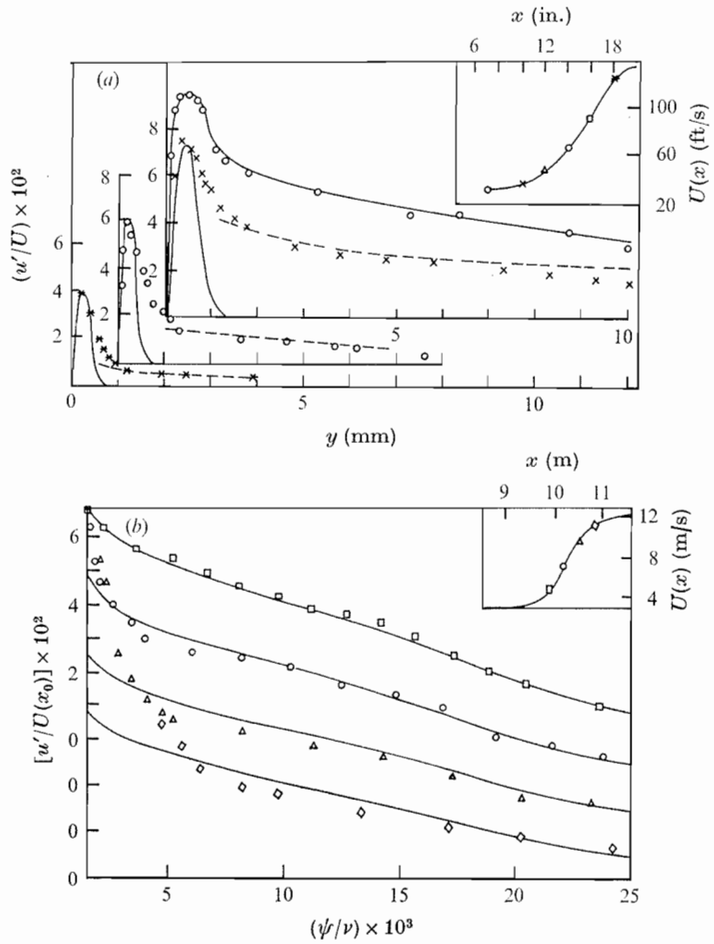

FIGURES 11(*a*, *b*). For legend see facing page.

(1969) and Blackwelder & Kovasznay (1972) respectively. A tentative application of the theory (which will be further discussed elsewhere) is therefore of interest, especially as other evidence regarding the relevance of rapid distortion to shear flow problems (Narasimha & Prabhu 1972) is also available.

On this basis, we may start with a u' profile assumed given at an initial station and compute its development downstream, applying rapid distortion theory along each streamline in the outer layer and the eigenfunction theory† described above in the inner layer. The results of such calculations are compared with measurements in figures 11(*a*) and (*b*): it will be seen that the agreement is generally very good, except in a narrow intermediate region where neither theory

† The exact eigenfunctions required have not been computed by us; we have followed an approximate procedure suggested by Kemp (unpublished report), the results of which compare well with the known exact solutions at $m = 0$ and $-0{\cdot}0476$. This same procedure incidentally gives (4.3) for the exponent in (4.2).

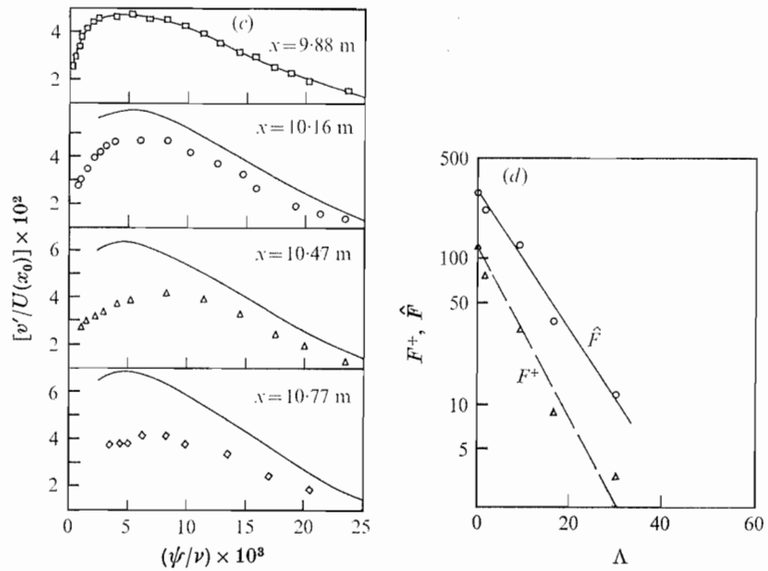

FIGURE 11. In (*a*), (*b*) and (*c*), the uppermost profile, drawn through the measured points, is taken as the initial condition for calculations. (*a*) Flow BR 3: u' normalized with local free-stream velocity; curves show laminar eigenfunctions (full lines) and rapid-distortion theory (broken lines). The same degree of agreement is obtained at all intermediate stations, omitted here for clarity. Inset indicates the relative positions of the measuring stations. (*b*) Flow BK: u' in outer region, normalized with reference free-stream velocity. Curves show rapid-distortion theory. Note shifts in the origin for the ordinate. (*c*) Flow BK: v' in outer region, normalized with reference free-stream velocity. Curves show rapid-distortion theory. Symbols same as in (*b*). (*d*) Bursting rate per unit span, in the flow SK; F^+, scaled in wall variables (broken line), and $\hat{F}$, scaled in mixed variables (full line). $\hat{F} = F^+(\frac{1}{2}R_{\delta^*}c_f)$.

will apply. (A formal matching of the two theoretical solutions does not appear possible since the outer solution does not possess a simple, well-defined inner limit.) It should perhaps be emphasized that these diagrams display the true decrease in u' that does occur during reversion. Earlier statements (Head & Bradshaw 1971; Blackwelder & Kovasznay 1972) that the absolute turbulence intensity q' remains nearly constant are correct in the rough sense that it does not keep in step with $U(x)$. Observation shows that, as the outer edge of the boundary layer is approached, q'^2 in fact increases roughly like U, consistent with rapid-distortion theory.

Rapid-distortion theory is less successful for the normal component v' (figure 11*c*), in this as in other shear flows. The precise reason for this is not known, but the vast difference in the turbulent scales in the x and y directions could be partly responsible. This is also reflected by the relatively better agreement with experiment of similar calculations for the spanwise component w' (not shown here), although even here it is not as good as for u'.

4.6. *Succession of events during reversion*

Many of the diagrams presented so far carry markers indicating the location of some of the following events:

K^*: $K \simeq 3 \times 10^{-6}$,

Δ^*: $\Delta_p \simeq -0{\cdot}025$,

L^*: disappearance of log region in wall law,

H^*: minimum in H,

u'^*: maximum in $u'_{\max}/U$,

u'^{**}: similarity in u' distributions,

W^*: wall parameters take quasi-laminar values,

Λ^*: $\Lambda \simeq 50$.

Does experiment show an orderly succession of these various events during reversion, or even a correlation among them? Examining the flows PH 1, BR 3 and BR 2, whose results are displayed in figures 7 (*b*), 8 (*a*) and 8 (*b*), the first four events in the above list are found to occur in the following order respectively: $L^*(K^*\Delta^*)H^*$, $K^*(L^*\Delta^*H^*)$ and $\Delta^*(K^*L^*H^*)$, events enclosed in parentheses all occurring at or very near the same measuring station. Although the above order cannot be accepted literally in the BR experiments (where the events are not always well separated, so that Δ^* is reported in BR 2 as occurring unreasonably† before L^*), the one definite conclusion that can be drawn is that H^* does not precede the other events, as has already been observed by Launder (1964). Furthermore, the point of departure of c_f from the fully turbulent curve is located close to Δ^* (figures 8 (*a*) and (*b*)).

On the other hand, the last four events in the list occur downstream of the first four. The general order appears to be $u'^*(W^*u'^{**}\Lambda^*)$, although u'^* cannot be well located in BR 3. The events W^* and Λ^* occur very close to each other also in all the experiments of Moretti & Kays analysed here. This aspect is further discussed in § 5.

It is interesting to re-examine the data on turbulent bursts in the light of the above picture. Their rate of occurrence F (per unit span) has been correlated with the parameter K by Kline *et al.* (1967), who deduce (by extrapolation) a critical value $K = 3{\cdot}5 \times 10^{-6}$ for the complete cessation of bursting and consequent relaminarization. Their data on the boundary layer for a 'strongly favourable pressure gradient' (designated SK in table 2) are shown plotted against Λ in figure 11 (*d*), using for F both the inner scaling suggested by Kline *et al.*,

$$F^+ = F\nu^2 U_*^{-3},$$

† If the equations of motion for a turbulent boundary layer are written in wall variables, it is found that the only non-dimensional parameter to appear is Δ_p, which should therefore show a strong correlation with violations of the law of the wall, as found by Patel (1965).

and a mixed scaling that Rao *et al.* (1971) have shown is more appropriate ($\hat{F} = F\nu\delta^*/UU_*$)†. Both parameters fall exponentially in Λ over the whole range of available data; no sharp critical station can be identified, nor can an obvious extrapolation to $F = 0$ be made. It will be seen that the maximum value of Λ attained in these experiments is only about 30, which from the above discussion would suggest that complete reversion has not taken place; this is supported by wall stress measurements, which show c_f still rising at the last station in the flow.

From the limited data available it would appear therefore that there is a rapid decline in the bursting rate in an accelerating turbulent boundary layer, well before the wall variables begin to assume quasi-laminar values‡. This view is consistent with the conclusions of Rao *et al.* (1971) that bursting rates are strongly influenced by the outer flow and are not exclusively wall phenomena.

4.7. *Retransition to turbulence*

In most of the experiments we have considered, the cycle of events is completed by retransition to fully turbulent flow. Launder (1964) has suggested that the process here must be largely similar to direct transition from laminar to turbulent flow, but the 'retransition point' (if it exists) has not been located in any of the experiments as definitely as it can be in direct transition (Dhawan & Narasimha 1958). The occurrence of a maximum in the shape factor H, sometimes taken to indicate retransition, is no more than a rough guide. We see, for example, in figure 7 (*b*) that the quasi-laminar theory is predicting flow development in PH 1 even beyond the maximum H, as satisfactorily as elsewhere.

The maintenance of an effectively laminar inner layer in spite of the highly disturbed state of the flow in the quasi-laminar region must be attributed to the strong stabilizing influence of the favourable pressure gradient. Correspondingly, we may expect retransition soon after the onset of instability. The critical instability Reynolds number for the inner layer can be estimated using the correlation given for example by Stuart in Rosenhead (1963, p. 543), in terms of the profile shape factor (for the inner layer, of course), which itself may be obtained by the Thwaites method (see § 3). A comparison with the computed values of the actual inner-layer Reynolds number is shown in figure 12 for three experiments. In PH 1 it would appear that the flow is still stable at the last measuring station, 2 in. downstream of the $H_{\max}$ point; the continued validity of the quasi-laminar solution (confirmed by figure 7 *b*) is therefore to be expected. In BR 2, the critical condition for instability is reached very near $H_{\max}$; c_f shows a strong departure (figure 8 *b*) from the quasi-laminar theory at the next station, unfortunately 6 in. downstream, showing that retransition certainly occurred

† Either scaling should be acceptable in this particular case, as the streamwise variation of R_θ is negligible in SK. For the same reason, correlation of the bursting rate with K could be useful in the particular flow SK.

‡ Although there is no information yet on the average bursting period $\bar{T}$ at a point in large favourable pressure gradients, note that an *increase* in $\bar{T}$ (as implied by data on F) would be significant, since in accelerating flow with a thinning boundary layer, we should expect a *decrease* in $\bar{T}$ ($\sim \delta/U$, according to Rao *et al.* 1971) if the boundary layer were in equilibrium.

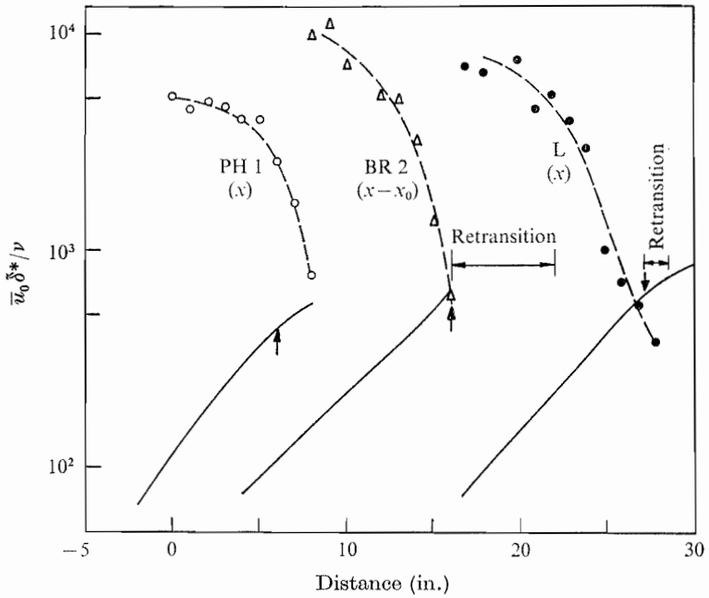

FIGURE 12. Determination of instability points for the inner layer. ——, quasi-laminar solution; – – –, critical Reynolds number for instability. Points from correlation of Stuart (Rosenhead 1963) with profile shape factor. Arrow marks location of maximum H.

before that station and quite possibly just downstream of instability. The sharpest location of retransition was made by Launder (1964) using Reynolds stress measurements; it will be seen that it correlates very well with our estimate of the onset of instability. Apparently the quasi-laminar flow is sufficiently disturbed that instability quickly triggers off sufficient energy production in the inner region to cause quick retransition.

Further evidence in support of this picture of retransition is contained in the observation of Blackwelder & Kovasznay (1972) that new turbulent spots are born near the wall ($8 < y^+ < 30$) when the pressure gradient has decreased sufficiently. Here and in the experiments of Moretti & Kays (1964) predictions of the quasi-laminar theory are in good agreement with measurement (of a sensitive parameter like c_f or S) right up to the calculated instability point for the inner layer.

5. Discussion

The dynamical considerations of § 4 suggest a more logical division of the flow into regions different from our preliminary attempt in § 1. In the first place, it is clear that the outer solution in the quasi-laminar limit is valid almost from the point of commencement x_0 of the pressure gradient; no transition region of type II can here be identified, and in a narrow but justifiable sense reversion in the outer layer can be said to occur immediately after the acceleration at x_0 in all the experiments reported to date.

On the other hand, the inner quasi-laminar solution, in particular for a wall parameter like c_f, is certainly not valid near x_0. However, the inner contributions to integral thicknesses like δ^* or θ are so small where they are incorrect (i.e. near x_0) that good estimates of R_θ and H can be made all the way from x_0. It is unfortunately not possible to use these estimates to infer from the momentum integral relation a value for c_f, which is a small difference between two large contributions to the momentum balance (note the strange similarity to adverse pressure gradient flows).

In fact the quasi-laminar solution for c_f appears to become useful only after the pressure-gradient parameter Λ reaches values of the order of 50; it is also around this same station in the flow that the intensity of the inherited turbulence begins to decay like a quasi-steady perturbation on a laminar boundary layer. It should be stressed that, in the present view of relaminarization as an asymptotic process, Λ cannot possess a 'critical' value; the number quoted above is rather a convenient indicator of the practical usefulness of the theory.

Further downstream, the inner layer becomes unstable as the pressure gradient decreases in severity; the evidence suggests that retransition quickly follows instability, the disturbed outer layer undoubtedly acting to reduce the gap between these two stages often noticed in careful experiments on direct transition.

The different stages in a reverting flow are possibly characterized best using c_f, whose variation is shown schematically in figure 13. Not much error is likely to be committed by assuming that the conventional turbulent laws are valid till Δ_p reaches the critical value of about $-0{\cdot}024$ used by Patel (1965). Beyond this point and before Λ reaches 50, c_f does not vary much, and the corresponding bubble-shaped region near the wall may be labelled as the true (reverse-) transitional region II in the flow. As a rough approximation, one is tempted to incorporate this region into a theoretical scheme by assuming c_f to be constant within II, at *either* the turbulent value at Δ^*, *or* the maximum from the quasi-laminar solution: the experimental data, summarized in table 3, encourage the speculation that the two values cannot be far from each other. (BR 1 and the PH experiments present certain difficulties, which are discussed in appendix C.) More refined approaches to the flow in this region must await careful measurements of c_f in boundary layers with high initial Reynolds numbers, but all the flows observed to date can be satisfactorily patched across II in the manner suggested to obtain a complete calculation of the whole flow.

This scheme must, however, be considered tentative in some respects, for the implicit assumption that Δ^* precedes Λ^* may not be universally valid. One can in fact conceive of conditions under which a calculation of the above sort would itself result (*a posteriori*) in Λ^* preceding Δ^*, although they involve appreciable changes in U over streamwise distances of the order of a few δ, so that the boundary-layer approximation itself becomes questionable. Nevertheless, this consideration emphasizes the need for further experimental work in flows with much higher initial Reynolds numbers than in current work, particularly to determine the relevant parameters in the reverse-transitional region and the role of Δ and Λ.

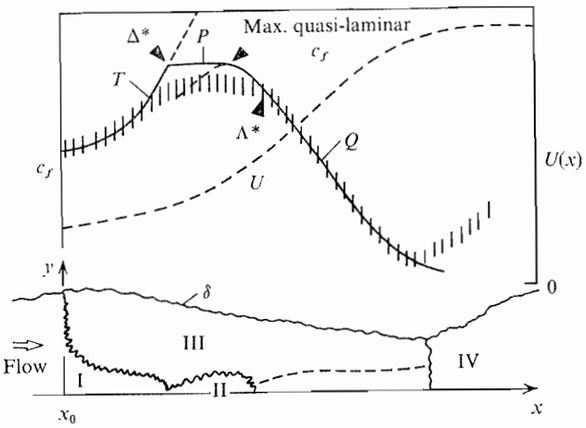

FIGURE 13. Schematic variation of skin-friction coefficient shown against different flow regimes during reversion. I, fully turbulent; II, reverse-transitional; III, quasi-laminar (dashed line separates inner and outer layers); IV, turbulent after retransition. Upper diagram compares variation of true c_f (shown hatched) with model suggested here, in which c_f follows fully turbulent theory (curve T) up to Δ^* and quasi-laminar theory (curve Q) beyond the point of maximum c_f. The gap between the two theories is patched by a region P of constant c_f; it is possible that the true c_f rises slightly above P, instead of always remaining lower as shown. Curves T and Q are shown dashed beyond their regions of validity.

Experiment	Maximum value from quasi-laminar theory	Measured c_f at Δ^*	Method of measurement
BR 1	0·0039	0·0058	Preston tube
BR 2	0·0064	0·0059	Heat-transfer gauge
BR 3	0·0062	0·0062	
BR 4	0·0039	0·0035–0·005	Preston tube (also Clauser plots)
BR 5	0·0046	0·004–0·0055	
BR 6	0·0054	0·005–0·006	
S 1	0·0045	0·0052	Clauser plot
PH 1	0·0037	0·00475	Fence technique
PH 2	0·0036	0·0043	

TABLE 3. Comparison of maximum value of c_f in quasi-laminar theory (computed using Thwaites's method) with measured value at the point Δ^*

In the final picture that emerges, only the reverse-transitional inner layer poses a difficult basic problem demanding further study, possibly based on modifications of the similarity arguments of Patel & Head (1968); but it does not strongly affect many important mean flow characteristics, which can be determined satisfactorily without invoking specific models for turbulence. Part of the reason for this is that the Reynolds shear stress, being nearly frozen, behaves in such a way it is are irrelevant to the mean flow dynamics. Perhaps this whole phenomenon, so largely governed by the need to conserve angular momentum

in a dominating pressure gradient, should only be called quasi-reversion: we suspect that it is quite common, and occurs in most good wind-tunnel contractions.

Part of this work was done while R.N. was visiting the University of Strathclyde: he would like to thank Professor Pack and his colleagues for their hospitality. K.R.S. acknowledges the award of a fellowship from the University Grants Commission. We are indebted to Dr P. A. Libby and Dr N. Kemp for correspondence on the eigenfunctions mentioned in §4.5.

Appendix A

Townsend's notion of equilibrium in the inner layer leads to the proposal (Townsend 1961, equation (3.9))

$$\frac{\partial u}{\partial y} = \frac{\tau^{\frac{1}{2}}}{ky}\left[1-\beta\frac{y}{\tau}\left|\frac{\partial \tau}{\partial y}\right|\right], \tag{A 1}$$

involving the parameters β and the Kármán constant k. Integrating for $u(y)$ we get

$$u^+ = \frac{u}{U_*} = \frac{1}{k}\left[\ln\left(\frac{4}{\Delta_\tau}\frac{(1+y^+\Delta_\tau)^{\frac{1}{2}}-1}{(1+y^+\Delta_\tau)^{\frac{1}{2}}+1}\right) + 2(1-\beta\,\mathrm{sgn}\,\Delta_\tau)\left((1+y^+\Delta_\tau)^{\frac{1}{2}}-1\right)\right] + B + 3{\cdot}7\Delta_p, \tag{A 2}$$

where $\mathrm{sgn}\,\Delta_\tau = \pm 1$ according as $\Delta_\tau \gtrless 0$: its appearance here, as in Townsend's inner law, is a consequence of the assumption that turbulent transport in equilibrium must occur down the gradient. The constant in (A 2) is evaluated following Patel & Head (1968), whose inner law differs from (A 2) solely through the absence of the $\mathrm{sgn}\,\Delta_\tau$ factor.

As no direct measurements of stress gradient in reverting flows have been reported, the only way of determining Δ_τ at present appears to be by making a best fit of the theoretical inner law to the experimental data. We have done this for flow PH 1, adopting both the Patel–Head version and equation (A 2) as the standard inner law and using $K = 0{\cdot}418$, $B = 5{\cdot}45$ and $\beta = 0{\cdot}18$ (as Patel & Head do). From the typical velocity profile comparisons shown in figure 14(*a*) it will be seen that Δ_τ cannot always be determined very accurately by this procedure, for the region available for judging the fit is only $y^+ < -1/\Delta_\tau$; beyond this point both inner laws lead to imaginary results.

Nevertheless, several interesting conclusions emerge from such calculations. First, the position where 'reversion' occurs, as judged by departure from the standard law, is the same according to either version. Second, the Δ_τ so found, like the more easily measured Δ_p, shows a maximum upstream of 'reversion', again irrespective of which inner law is used (figure 14(*b*)). Thus one is forced to admit regions of 'fully turbulent' flow where Δ_τ has reached and passed the 'critical' value at which 'reversion' eventually takes place; at least, then, there must be one more parameter in the problem.†

† In addition to the two already present in the inner law, namely Δ_τ and Δ_p, although the latter does not contribute significantly to u^+.

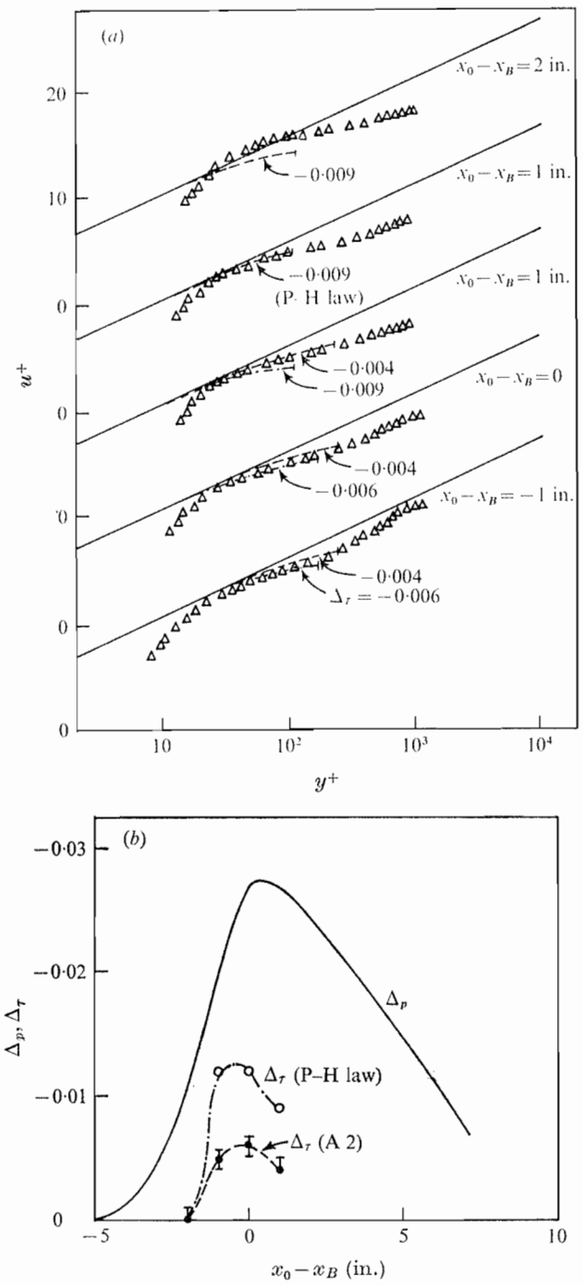

FIGURE 14. (*a*) Determination of Δ_τ by fitting inner law (A 2) to measured velocity profiles in flow PH 1. At $x_0-x_B=0, -1$ in., curves for two different values of Δ_τ are drawn, to show the likely error in obtaining Δ_τ. At $x_0-x_B=1$ in., both the Patel–Head inner law and (A 2) are shown with $\Delta_\tau=-0{\cdot}009$ (the critical value quoted by Patel & Head); using (A 2), Δ_τ is seen to be about $-0{\cdot}004$ at this station. At $x_0-x_B=2$ in., the inner law (A 2) is shown with $\Delta_\tau=-0{\cdot}009$ for illustration, but no value of Δ_τ will fit the measurements. (*b*) The parameters Δ_p and Δ_τ. —·—·—, Δ_τ from Patel–Head law; – – –, Δ_τ from (A 2). For $x_0-x_B\geqslant 2$ in. no value of Δ_τ produces agreement with experiment. (x_0-x_B as in Patel & Head 1968.)

Finally, the numerical value of Δ_τ inferred from this procedure depends appreciably on which version of the inner law is used: thus the final 'critical' value for Δ_τ is only about $-0{\cdot}004$ using (A 2), as against $-0{\cdot}009$ using the Patel–Head version. It would be difficult to reconcile the former value with the criterion of Bradshaw (1969).

We conclude from all this that the inner law in a turbulent boundary layer subjected to favourable pressure gradients is not sufficiently well established for departures from it to be interpreted as evidence of reversion.

Appendix B

Equation (3.7) when written in full reads

$$n'(x)=\frac{U'}{U}\left[-\frac{1-U_0^2}{U_0}\left(\frac{B_1B_2}{B_3}+B_4\right)+(3B_1-B_5)\right]\Big/\left(\frac{B_1B_6}{B_3}+B_7\right),$$

where the $B_i=B_i(U_0,n)$ are the following functions:

$$B_1=\frac{(1-U_0)(1-2U_0)}{n+1}+U_0(1-U_0)-\frac{(1-U_0)^2}{2n+1},$$

$$B_2=3U_0^2-1+\frac{1+6U_0-9U_0^2}{n+1}+\frac{3(1-U_0)(1-3U_0)}{2n+1}-\frac{3(1-U_0)^2}{3n+1},$$

$$B_3=U_0(1-U_0^2)+\frac{(1-U_0)(1-3U_0^2)}{n+1}-\frac{3U_0(1-U_0)^2}{2n+1}-\frac{(1-U_0)^3}{3n+1},$$

$$B_4=1-2U_0+\frac{4U_0-3}{n+1}+\frac{2(1-U_0)}{2n+1},$$

$$B_5=2B_1+n(1-U_0)/(n+1),$$

$$B_6=-\left[\frac{(1-U_0)(3U_0^2-1)}{(n+1)^2}+\frac{6U_0(1-U_0)^2}{(2n+1)^2}+\frac{3(1-U_0)^3}{(3n+1)^2}\right],$$

$$B_7=-\frac{(1-U_0)(1-2U_0)}{(n+1)^2}+\frac{2(1-U_0)^2}{(2n+1)^2}.$$

Appendix C

The difficulties presented by the PH experiments and by BR 1 during the analysis of the flows listed in table 2 are discussed here.

PH experiments. Quasi-laminar calculations of § 3 do not agree with measurement in PH 2, but the reason could be that PH 2 is not a plane boundary layer as may be inferred from the fact that the data do not obey the two-dimensional momentum integral equation (Sreenivasan 1972*a*): the experiment was conducted in a pipe whose radius was only twice the initial boundary-layer thickness. Further, there are comparable changes in the flow along both axial and radial directions during acceleration, so that the applicability of the boundary-layer approximation may itself well be in doubt. Finally, the measurements were made at a fixed station while the pressure gradient was translated, so that the origin x_0 and the state of the flow there were not the same during the experiment.

These factors do not necessarily invalidate the study of the inner layer that was the chief concern of Patel & Head; and the first two factors do not operate as severely in PH 1, which has a thinner boundary layer and is tolerably plane. However, for $x-x_0 > 4$ in. R_θ calculated by integrating the two-dimensional momentum integral equation is always more (by 10–20 %) than the measured value. Correcting for the axisymmetry of the flow in the definitions of momentum and displacement thickness does not materially affect this observation. On the other hand, use of the theoretical quasi-laminar c_f instead of the measured value in integrating the equation, with all other quantities still uncorrected for axisymmetry, results in much closer agreement (maximum deviation $\simeq 5$ %) in the same region, a result which goes some distance in reinforcing the accuracy of the quasi-laminar calculations. Finally, if one uses the quasi-laminar c_f and corrected values for the boundary-layer parameters, this agreement remains substantially the same; the remaining small discrepancies could well be the effect of varying initial conditions.

Experiment BR 1. For this flow, detailed comparison with experiment shows that the quasi-laminar shape factor continues to increase for some distance downstream of the point where the reported experimental values start decreasing. A closer look at the raw data of BR 1 (which incidentally was a preliminary experiment that preceded by several months the other flows reported in Badri Narayanan & Ramjee 1969) revealed certain inconsistencies which could not be completely explained (we are grateful to these authors for a very detailed discussion of the flow). However, a repetition of the experiment with the same apparatus and very nearly the same conditions yielded results quite consistent with the quasi-laminar theory.

REFERENCES

Back, L. H., Massier, P. F. & Gier, H. L. 1964 *Int. J. Heat Mass Trans.* **7**, 549.

Back, L. H. & Seban, R. A. 1967 *Proc. Heat Trans. Fluid Mech. Inst.* **20**, 410.

Badri Narayanan, M. A. & Ramjee, V. 1969 *J. Fluid Mech.* **35**, 225.

Batchelor, G. K. & Proudman, I. 1954 *Quart. J. Mech. Appl. Math.* **7**, 83.

Blackwelder, R. F. & Kovasznay, L. S. G. 1972 *J. Fluid Mech.* **53**, 61.

Bradshaw, P. 1969 *J. Fluid Mech.* **35**, 387.

Chen, K. K. & Libby, P. A. 1968 *J. Fluid Mech.* **33**, 273.

Coles, D. 1953 *Jet Propulsion Lab., Caltech. Rep.* no. 20–69.

Curle, N. 1962 *The Laminar Boundary Layer Equations.* Oxford University Press.

Dhawan, S. & Narasimha, R. 1958 *J. Fluid Mech.* **3**, 418.

Head, M. R. & Bradshaw, P. 1971 *J. Fluid Mech.* **46**, 385.

Jones, W. P. & Launder, B. E. 1972 *J. Fluid Mech.* **56**, 337.

Kline, S. J., Moffatt, H. K. & Morkovin, M. V. 1969 *J. Fluid Mech.* **36**, 481.

Kline, S. J., Reynolds, W. C., Schraub, F. A. & Runstadler, P. W. 1967 *J. Fluid Mech.* **30**, 741.

Launder, B. E. 1964 *Gas Turbine Lab., M.I.T. Rep.* no. 77.

Launder, B. E. & Stinchcombe, H. S. 1967 *Mech. Engng Dept., Imperial College Rep.* TWF/TN/21.

Lighthill, M. J. 1950 *Proc. Roy. Soc.* A **202**, 359.

Moretti, P. H. & Kays, W. M. 1964 *Thermosci. Mech. Engng Dept., Stanford University Rep.* PG-1.

Moretti, P. H. & Kays, W. M. 1965 *Int. J. Heat Mass Trans.* **8**, 1187.

Narasimha, R. & Prabhu, A. 1972 *J. Fluid Mech.* **54**, 1.

Patel, V. C. 1965 *J. Fluid Mech.* **23**, 185.

Patel, V. C. & Head, M. R. 1968 *J. Fluid Mech.* **34**, 371.

Ralston, A. & Wilf, H. S. (eds.) 1960 *Mathematical Methods for Digital Computers.* Wiley.

Ramjee, V. 1968 Ph.D. thesis, Department of Aeronautical Engineering, Indian Institute of Science.

Rao, K. N., Narasimha, R. & Badri Narayanan, M. A. 1971 *J. Fluid Mech.* **48**, 33.

Rosenhead, L. (ed.) 1963 *Laminar Boundary Layers.* Oxford University Press.

Schraub, F. A. & Kline, S. J. 1965 *Thermosci. Div. Mech. Engng Dept., Stanford University Rep.* MD-12.

Spence, D. 1956 *J. Aero. Sci.* **23**, 3.

Sreenivasan, K. R. 1972*a* *Dept. Aeron. Engng, Ind. Inst. Sci. Rep.* 72 FM2.

Sreenivasan, K. R. 1972*b* *Dept. Aeron. Engng, Ind. Inst. Sci. Rep.* 72 FM 7.

Sreenivasan, K. R. & Narasimha, R. 1971 *Dept. Aeron. Engng, Ind. Inst. Sci. Rep.* 71 FM 11.

Stratford, B. S. 1959 *J. Fluid Mech.* **5**, 1.

Taylor, G. I. 1929 *Proc. Roy. Soc.* A **124**, 243.

Thwaites, B. 1949 *Aero. Quart.* **1**, 245.

Townsend, A. A. 1956 *The Structure of Turbulent Shear Flow.* Cambridge University Press.

Townsend, A. A. 1961 *J. Fluid Mech.* **11**, 97.

Van Dyke, M. 1964 *Perturbation Methods in Fluid Mechanics.* Academic.

Vivekanandan, R. 1963 M.Sc. thesis, Department of Aeronautical Engineering, Indian Institute of Science.